J Mater Sci (2009) 44:2162–2166
DOI 10.1007/s10853-009-3370-6

LETTER

Improved magnetoelectric properties of piezoelectric–magnetostrictive nanocomposites synthesized using high-pressure compaction technique

Vishwas Bedekar · Narayan Poudyal · Chuan-bing Rong · J. Ping Liu · Choong-Un Kim · Shashank Priya

Received: 11 December 2008 / Accepted: 23 February 2009 / Published online: 8 March 2009

Introduction

Magnetoelectric (ME) effect results in polarization of material with applied magnetic field and magnetic field induction with an applied electric field. ME composites with particulate structure show lower magnitude of ME coefficient as compared to that of laminate composites [1–10]. However, the advantages of particulate composites are simpler and cheaper synthesis technique, availability of wide range of compositions, scalability, and presence of both direct and converse ME effect. Thus, there has been continuous emphasis on enhancing the magnitude of particulate composites [11, 12]. In this letter, we report the properties of particulate composites synthesized using: (1) high-pressure compaction sintering technique and (2) conventional technique. The results clearly show that high-pressure sintering technique results in improved ME coefficient. We also study the effect of ratio of piezoelectric and magnetostrictive phase in the core-shell nanoparticles which are used to synthesize high-pressure sintered composites. The advantage of using core-shell particles in comparison to individual piezoelectric and magnetostrictive particles for synthesizing composite is that it results in controlled distribution of one phase with respect to other. This preserves the individual electrical and magnetic properties of each phase.

V. Bedekar · C.-U. Kim
Department of Materials Science and Engineering, UT Arlington, Arlington, TX 76019, USA

N. Poudyal · C.-b. Rong · J. P. Liu
Department of Physics, UT Arlington, Arlington, TX 76019, USA

S. Priya (✉)
Department of Materials Science and Engineering, Virginia Tech, Blacksburg, VA 24061, USA
e-mail: spriya@vt.edu

Experimental procedure

The synthesis of nickel ferrite (NFO) nanoparticles was performed by standard airless chemical synthesis technique in a nitrogen atmosphere. The reagents were obtained from commercial sources (Sigma-Aldrich, Inc.) and used without further purification. In a typical synthesis of 18-nm NFO nanoparticles, a mixture of 1 mmol of Ni-II (acetyl acetonate) and 2 mmol of 1,2-hexadecanediol (HDD) was added to a 125-mL European flask containing a magnetic stir bar. Benzyl ether (BE, 20 mL) was then transferred to the flask and the contents were stirred while purging with N_2 for 20 min at room temperature. The flask was heated to 120 °C for 20 min and 1.5 mmol of iron pentacarbonyl [$Fe(CO)_5$] was injected into the flask while continuing the N_2 purge. After 3 min, 5 mmol each of oleic acid and oleylamine were injected and the mixture was maintained under N_2 blanket and heated to 160 °C at a rate of 5 °C/min for 10 min. Next, the flask was heated to the refluxing temperature of 295 °C for 30 min before cooling down to room temperature under the N_2 blanket. Size of the $NiFe_2O_4$ (NFO) nanoparticles was controlled well by varying the solvents, amount of surfactants, and heating rates. For example, when BE was replaced by phenyl ether while keeping other reaction parameters unchanged, particles size was reduced from 18 to 6 nm. If BE was used as solvent and amount of both the surfactants were increased from 5 to 10 mmol, the size of the particles was increased from 18 to 22 nm. TEM images and X-ray diffraction patterns of the as-synthesized particles are shown in Fig. 1a–d.

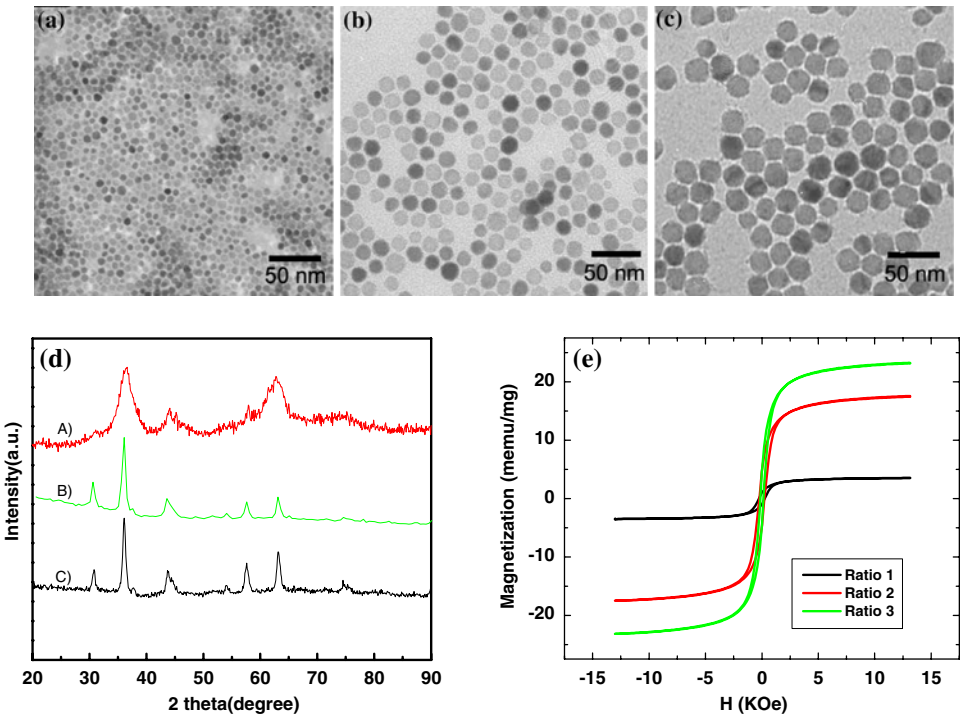

Fig. 1 **a–c** TEM image of the NFO particles with varying particle size. **d** X-ray diffraction pattern of the nanoparticles. **e** Magnetic properties of PZT/NFO nanoparticles

Piezoelectric particles were synthesized corresponding to formulation $0.8[Pb(Zr_{0.52}Ti_{0.48})O_3]–0.2[Pb(Zn_{1/3}Nb_{2/3})O_3]$ (PZT) using conventional mixed oxide route. Coating of NFO nanoparticles on PZT was performed by chemical synthesis method following the procedure described above with addition of PZT particles, as seeds, that were coated after the procedure. Keeping the PZT concentration constant at 6.1 mmol, NFO concentration was increased twice and thrice to obtain Schemes 2 and 3, respectively. Hence, molar ratios of PZT to NFO precursors are 2.44:1, 1.22:1, and 0.81:1 for Schemes 1, 2, and 3, respectively. Table 1 shows the three different schemes of NFO/PZT solution used to synthesize the composite particles. The particle size of NFO was 22 nm for all the schemes. Magnetic properties of as-synthesized particles with Schemes 1, 2, and 3 are shown in Fig. 1e. As the amount of magnetic phase increases, the magnetic moment and magnetization increases from 3.50 memu/mg for Scheme 1 to 17.40 memu/mg for Scheme 2 and 23.13 memu/mg for Scheme 3.

Results and discussion

To investigate the effect of NFO–PZT ratio, the coated particles were used to synthesize the particulate composite structure. Pellets of three different schemes were pressed in a 0.25-in. die under hydraulic pressure of 2 kpsi followed by cold isostatic pressure of 30 kpsi. Thin layers of PZT were pressed on top of the pellets to increase the resistivity. The samples were then sintered at 1040 °C for 3 h under a 150 g weight. All the recovered samples were bi-layered, with one layer each of PZT and PZT–NFO with thickness 0.4 mm. The grain size was found to reduce with increasing NFO concentration in the composite. The composite with Scheme 1 was found to exhibit uniform and dense microstructure while composites with Schemes 2 and 3 had presence of porosity. Figure 2 shows the variation of ME coefficient as a function of DC bias field for three different schemes. Sample with Scheme 1 shows the highest ME coefficient of the order of 105 mV/cm Oe at 500 Oe DC

Table 1 Variation of PZT to NFO coating in the composite nanoparticles

	PZT (mmol)	Ni (II) (acetyl acetonate) (mmol)	1,2-Hexadecanediol (mmol)	Benzyl ether (mL)	Iron pentacarbonyl (mmol)	Oleic acid (mmol)	Oleyl amine (mmol)
Scheme 1	6.1	1	1	20	1.5	5	5
Scheme 2	6.1	2	2	50	3	10	10
Scheme 3	6.1	3	3	60	4.5	15	15

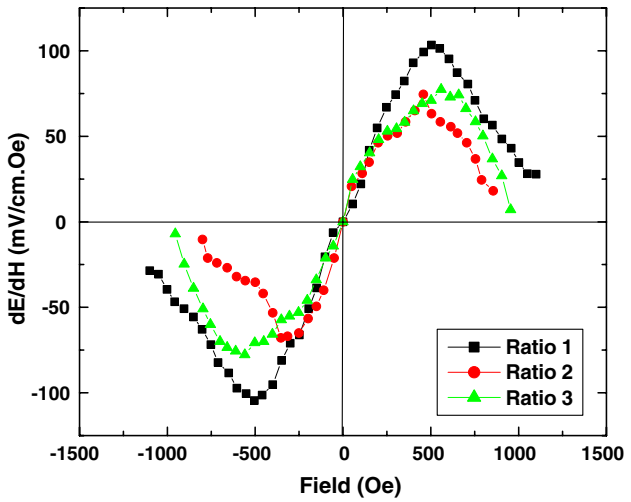

Fig. 2 Magnetoelectric coefficient of the composites with three different schemes as shown in Table 1. The ratio of PZT to NFO decreases from Scheme 1 to 3

bias field. Thus, composite nanoparticles of Scheme 1 were used for high-pressure sintering experiments.

High-pressure sintering was conducted to achieve homogenous microstructure with ordered distribution of NFO phase. PZT–NFO composite particles were pressed using a 0.25-in. disc-shaped die at 2 kpsi and sintered at 1 GPa and 600 °C for 30 min using Rockland SV-TC high compaction machine. After sintering, the bi-layer sample was removed from the metal die using a coarse file. The thickness of PZT–NFO layer in this bi-layer composite was 0.2 mm. The sample was then annealed at 1040 °C for 3 h, electroded, and, subsequently, poled at 2.5 kV/mm in silicon oil bath at 120 °C for 30 min. This sample was measured to have a longitudinal piezoelectric coefficient of 164 pC/N, dielectric constant of 880, and dielectric loss factor of 1.4%. Figure 3a and b shows the TEM bright-field (BF) and dark-field (DF) image of PZT–NFO-sintered composite. The contrast clearly shows the presence of NFO phase (dark spots at BF) on the bigger PZT grains. SAED pattern indicates the presence of NFO (111) phase with some arc formation in the ring diffraction pattern. The arcs suggest minor texturing effect of NFO phase for some of the grains in the area under investigation. These NFO fragments are fully crystallized after the sintering and annealing process. Based upon the TEM analysis, the microstructure of the composite is schematically depicted in Fig. 3c. The microstructure reveals well-grown PZT grains with NFO clusters dispersed along the initial grain boundary formed during high-pressure compaction. These NFO clusters migrate from the initial location resulting in mixed orientation of NFO phase at the initial grain boundaries of PZT grains as well as randomly dispersed NFO islands on PZT grains.

Figure 4 shows the variation of ME coefficient as a function of DC bias field for the composite sample synthesized by high-pressure compaction sintering technique. The peak ME coefficient of 187 mV/cm Oe was found at 285 Oe DC bias field. The result clearly shows that high-pressure compaction results in enhanced ME coefficient compared to the conventionally sintered samples. This enhancement may be correlated to partially ordered distribution of NFO particles with specific orientation along the PZT grains as shown in Fig. 3c. Piezoelectric grains in this microstructure are expected to be under finite compressive strain due to difference in volume of unit cell between spinel and perovskite phase. The lattice parameter

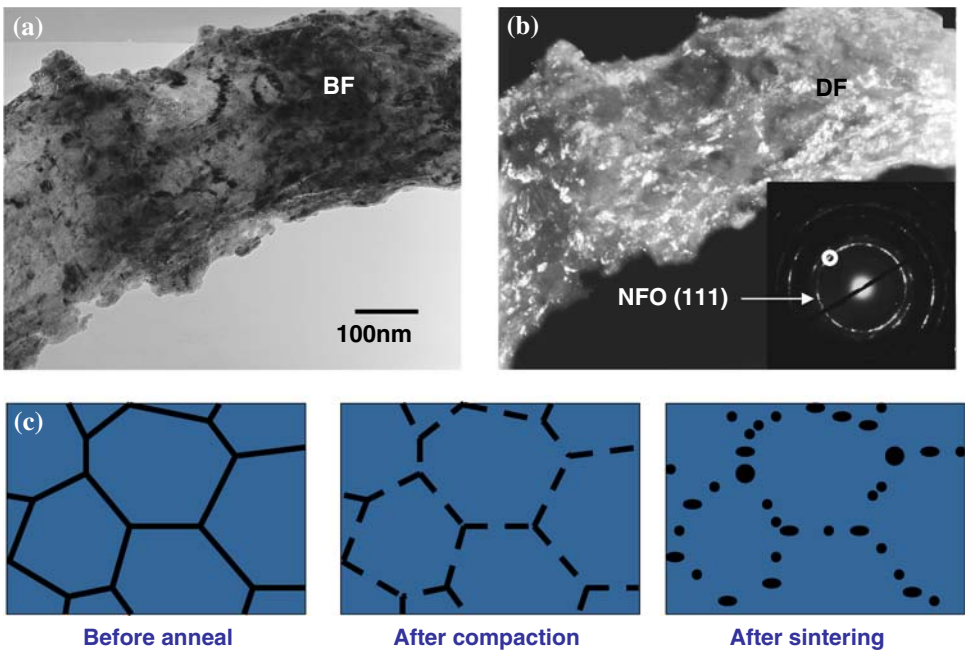

Fig. 3 TEM analysis of the high-pressure compacted nanocomposite. **a** Bright-field image. **b** Dark-field image. **c** Schematic illustration of the microstructure under high-pressure compaction. The dark-field image is taken from the NFO (111) diffraction spot (*circled area*) and, therefore, not all NFO phases is visible as white contrast

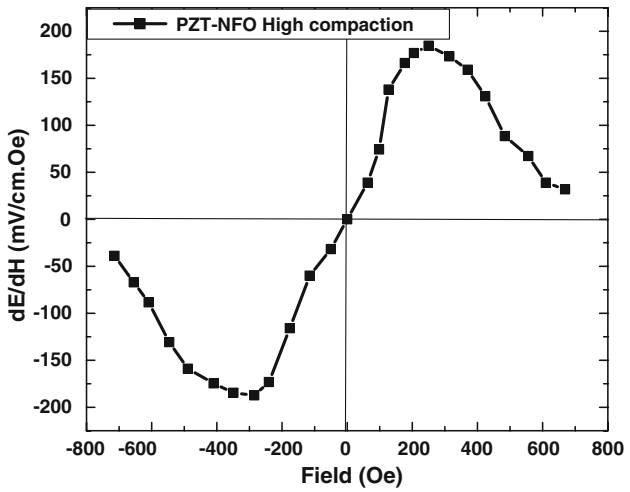

Fig. 4 Magnetoelectric coefficient as a function of DC bias field for the high-pressure compaction-sintered sample

of PZT in particulate-sintered composite sample of Mn-modified NFO (NFM) and PZT was measured to be $a^{s}_{pzt} = 3.87$ Å and $c^{s}_{pzt} = 4.07$ Å with $c/a = 1.052$ while NFM as $a_{NFM} = 8.42$ Å, resulting in a $\sim$8% lattice mismatch between the two structures [13]. However, by synthesizing those in composite form such that the phase separation occurs at grain boundaries may accommodate this strain through the creation of misfit dislocations which will provide improved bonding. Dislocations' lifting the incoherency relieves the total internal strain through partially ordered distribution of the NFO phase along the boundary whose width will be determined by the change in free energy of the system with and without ordering of NFO and its shape factor. In conventional particulate-sintered composites consisting of magnetostrictive and piezoelectric grains, the interfacial defects are distributed throughout the microstructure resulting in porosity and heterogeneity. This drawback can be overcome by synthesizing the microstructure shown in Fig. 3.

In addition, the ordered distribution of NFO phase will preserve the physical properties of piezoelectric and magnetostrictive phase. In particulate-sintered composites consisting of random distribution of magnetostrictive particles, there is excessive cross-diffusion of ions across the interface. Recently, it was shown in Cu-modified nickel zinc ferrite (NCZF)–PZNT composites that Cu ions diffuse into PZNT while Pb ions diffuse into NCZF [14]. This cross-diffusion lowers the magnitude of magnetostrictive constant and piezoelectric voltage constant. Another drawback of particulate-sintered composites is connectivity of the ferrite particles which lowers the overall resistivity and reduces the poling voltage. However, by confining the distribution of NFO along the grain boundaries and controlling the fraction of such boundaries, higher poling voltage can be applied.

Recent results by Grössinger et al. on composite consisting of 50% cobalt ferrite–50% barium titanate in "core-shell" structure shows 20 times larger magnetoelectric coefficient as compared to randomly dispersed composites [15]. The results were analyzed in terms of coupling coefficient k, given as $k_{par} = \lambda_{par} d\lambda_{par}/dH$, where λ_{par} represents the longitudinal magnetostriction, H is the applied magnetic field, and d is the effective sample thickness. It was shown that magnitude of ME coefficient increases with k which is higher for core-shell structure. These results are consistent with our own data which shows that core-shell $Pb(Zr,Ti)O_3$ (PZT)–$NiFe_2O_4$ (NF) particulate nanocomposites provide higher magnitude of ME coefficient [16]. In this case, core-shell composite resulted in good interface bonding and effective strain transfer across the interface. These prior results further indicate that the microstructure in Fig. 3, which has a resemblance to core-shell structure, can provide effective elastic coupling between the magnetostrictive and piezoelectric phases. The magnitude of magnetostriction coefficient, $\lambda_{par,}$ and k will be higher for the NFO-ordered phase distribution along the grain boundaries due to texturing and phase separation.

Conclusion

In summary, this letter reports the high-compaction sintering technique of PZT–NFO nano core-shell structure to form a dense ME particulate composite. The results show that high-compaction sintering technique can provide large magnetoelectric coupling. In addition, it was shown that composites corresponding to formulation 1:1 (Scheme 1) have the highest magnetoelectric coefficient which could be related to higher resistivity and dense microstructure for equivalent fraction of piezoelectric and magnetostrictive particles.

Acknowledegement The authors gratefully acknowledge the financial support from Army Research Office.

References

1. Suchetelene JV (1972) Philips Res Rep 27:28
2. Harshe GR (1991) Magnetoelectric effect in piezoelectric–magnetostrictive composite. Ph.D. Dissertation, Pennsylvania State University, University Park, PA
3. Srinivasan G, Rasmussen E, Levin B, Hayes R (2002) Phys Rev B 65:134402
4. Lalestin U, Padubnaya N, Srinivasan G, Devreugd CP (2004) Appl Phys A Mater Sci Process 78(1):33
5. Dong SX, Zhai J, Li JF, Viehland D (2006) J Appl Phys 88:082907
6. Dong SX, Li JF, Viehland D (2003) IEEE Trans Ultrason Ferroelectr Freq Control 50:1253

7. Dong SX, Li JF, Viehland D (2004) J Appl Phys 96:3382
8. Dong SX, Cheng J, Li JF, Viehland D (2003) Appl Phys Lett 83:4812
9. Dong SX, Li JF, Viehland D (2004) Appl Phys Lett 85:3534
10. Ryu J, Priya S, Uchino K (2002) J Electroceram 8:107
11. Islam RA, Priya S (2008) J Mater Sci 43:3560. doi:10.1007/s10853-008-2562-9
12. Islam RA, Viehland D, Priya S (2008) J Mater Sci Lett 43:1497
13. Islam R, Jiang J, Bai F, Viehland D, Priya S (2007) Appl Phys Lett 9:162905
14. Islam R, Rong C, Liu JP, Priya S (2008) J Mater Sci Lett 43:6337
15. Grössinger R, Duong GV, Sato-Turtelli R (2008) J Magn Magn Mater 320:1972
16. Islam RA, Bedekar V, Poudyal N, Liu JP, Priya S (2008) J Appl Phys 104:104111